Pharmaceutical Research, Vol. 25, No. 8, August 2008 (© 2007)
DOI: 10.1007/s11095-007-9489-8

Research Paper

Semi-mechanistic Pharmacokinetic/Pharmacodynamic Modelling of the Antinociceptive Response in the Presence of Competitive Antagonism: The Interaction Between Tramadol and its Active Metabolite on μ-Opioid Agonism and Monoamine Reuptake Inhibition, in the Rat

Horst Beier,[1] María J. Garrido,[2] Thomas Christoph,[3] Dirk Kasel,[1] and Iñaki F. Trocóniz[2,4]

Received June 25, 2007; accepted October 23, 2007; published online November 16, 2007

Purpose. To establish a semi-mechanistic pharmacokinetic/pharmacodynamic (pk/pd) model for racemic tramadol (T) integrating all the components with a significant contribution to T effects in rats, using cold allodynia in the Bennett model of neuropathic pain.
Methods. Male Sprague-Dawley rats (n=53) were randomly allocated in six groups receiving saline, racemic T (5 mg/kg), RR-T (5 mg/kg), SS-T (5 mg/kg), RR-*O*-demethyltramadol [RR-M1 (1 mg/kg)] or SS-M1 (30 mg/kg) in two h intravenous infusion.
Results. The μ-opioid effects of RR-M1 ($E_{RR\text{-}M1}$) were described with an effect compartment model. Contribution to analgesic response of RR-T resulted negligible. The monoamine re-uptake inhibition effects ($E_{SS\text{-}M1,T}$) were modelled as an indirect response model incorporating a competitive interaction between SS-T and SS-M1. $E_{RR\text{-}M1}$ and $E_{SS\text{-}M1,T}$ were finally considered as a two independent stimuli converging into a single and common antinoceptive stimulus. The estimates of the steady-state plasma concentrations eliciting half of maximum response for RR-M1, SS-T, and SS-M1 were 20.2, 230, and 869 ng/ml, respectively. RR-M1 is the main active component, but SS-T having a significant contribution.
Conclusion. Cold allodynia in the Bennett model has proven an adequate experimental set up to develop complex pk/pd models in analgesia involving different mechanisms of action.

KEY WORDS: neuropathic pain; racemic tramadol; rat model; semi-mechanistic pharmacokinetic/pharmacodynamic model.

INTRODUCTION

Tramadol (T), an analgesic compound administered as a racemic mixture of RR-tramadol (RR-T) and SS-tramadol (SS-T), which produces among others the active RR-*O*-demethtyltramadol (RR-M1) and SS-*O*-demethyltramadol (SS-M1) metabolites, has been classified as an "atypical" opiod drug (1). T combines the μ-opioid related effects elicited mainly by RR-M1 and the monoamine re-uptake inhibition effects attributed to SS-T and SS-M1 (2–4).

During the last decade the nature of the pharmacodynamic (pd) interactions between the μ-opiod and monoamine re-uptake inhibition mechanisms was studied *in vivo* in different pain animal models (5,6). More recently, the pharmacokinetic/pharmacodynamic (pk/pd) relationships were established for RR-M1 and SS-M1 (4,7), and RR-T (8), using tail-flick. One of the disadvantages of tail-flick as antinociceptive model is due to its limitation to reflect non-opiod mediated effects such as the monoamine re-uptake inhibition (9). More recently, the analgesic effects of T have been described in the paediatric population using a pk/pd model (10). Although in that article the authors identified both racemic T and racemic M1 as active components, an interaction pd model combining the effects of T and M1 could not be established. T is still a matter of active research, for example, it has been suggested as a new probe for cytochrome P450 2D6 phenotyping (11) and in a recent study (12), the analgesic effects of T were decreased after co-administration of paroxetine (a cytochrome P450 2D6 inhibitor) confirming again that M1 is an important element of T activity (13). To date a mechanistic pk/pd model addressing

[1] Department of Pharmacokinetics, Grünenthal GmbH, 52078, Aachen, Germany.
[2] Department of Pharmacy and Pharmaceutical Technology, School of Pharmacy, University of Navarra, Apartado 177, Pamplona, 31080, Spain.
[3] Department of Pharmacology, Grünenthal GmbH, 52078, Aachen, Germany.
[4] To whom correspondence should be addressed. (e-mail: itroconiz@unav.es)

ABBREVIATIONS: $E_{RR\text{-}M1}$, $E_{SS\text{-}M1}$, $E_{SS\text{-}T}$, $E_{SS\text{-}M1,T}$, E_{RRSS}, 0-1 normalized antinociceptive stimuli elicited by RR-M1, SS-M1, the combination of SS-T and SS-M1, and the interaction between the μ-opioid and monoamine re-uptake inhibition mechanisms, respectively; k_{e0}, first order rate constant governing the equilibrium in the distribution between plasma and biophase; k_{in}, and k_{out} are the zero, and first order rate constants of release and re-uptake of noradrenaline, respectively; M1, *O*-demethyltramadol; RR-M1, RR-*O*-demethyltramadol; RR-T, RR-Tramadol; SS-M1, SS-*O*-demethyltramadol; SS-T, SS-Tramadol; T, racemic tramadol.

the different contribution of the enantiomers of T and the active metabolite M1 has not been established yet.

On the basis of those considerations, the objective of the current study was to establish a semi-mechanistic pk/pd model for tramadol integrating all the components with a significant contribution to tramadol effects. To achieve this goal we have used the Bennett cold plate test as the animal pain model, which has been shown to be adequate to capture opioid and non-opioid mechanisms (9,14). This model was adapted to fit into an automated blood-sampling device providing simultaneous pharmacokinetics (pk) and pd information in each animal. In order to reduce the impact of blood sampling on the pharmacological observations, blood samples were taken 5 min after the pharmacological observations.

MATERIALS AND METHODS

Chemicals and Material

T, RR-T, SS-T, RR-M1, and SS-M1 were provided by Grünenthal GmbH (Aachen, Germany). Medetomidin was purchased from Pfizer, Dormicum from Roche and Fentanyl sulphate from Synopharm. Na-heparin (Liquemin®) was obtained from Hoffmann-La Roche AG (Grenzach-Wyhlen, Germany). The catheters were purchased from BASi (West Lafayette, USA).

Experimental Design

Fifty three male Sprague-Dawley rats weighing 240±47 g were randomly allocated in six groups receiving saline, T (5 mg/kg), RR-T (5 mg/kg), SS-T (5 mg/kg), RR-M1 (1 mg/kg) or SS-M1 (30 mg/kg) in 2 h intravenous infusion. The protocol was approved by the regional animal ethics committee according to the german law of animal welfare (no. FG-PK-99-22).

Animal Preparation

In a first surgery the rats underwent a constriction of the right common sciatic nerve according to Bennett and Xie, (15) under pentobarbital (60 mg/kg i.p.) anaesthesia. The sciatic nerve was exposed by blunt dissection at the level of mid-thigh, and four loose ligatures (softcat®chrom USP 4/0, metric2; Braun Melsungen, FRG) were placed around the nerve taking care not to interrupt the epineural circulation. Within 1 week the rats developed cold allodynia in the ipsilateral hind paw which is stable over several weeks (16). Animals were kept at laboratory standard conditions of 22–25°C and a relative humidity of 30–70%. They were acclimatized for at least 5 days. Food and water were provided *ad libitum*.

Three to four days before administration of the test compound, a catheter was implanted into the femoral vein contralateral to the ligation site for substance administration and a second one, was implanted into the carotid artery for blood sampling. Surgery was performed under anaesthesia using Medetomidin (0.15 mg/kg), Dormicum (Midazolam, 2.0 mg/kg) and Fentanyl (0.005 mg/kg). Directly after the surgery, the rats were placed in the RATURN® cages of the Culex® automated blood sampling device (ABS; BASi, West Lafayette, USA). The arterial catheter was connected to the tubings of the ABS. The intravenous catheter was connected to EMPIS® infusion pumps (BASi, West Lafayette, USA). To prevent blood clotting the catheters were flushed with system liquid (isotonic saline with 10 U heparin/ml) every 8 min. Both systems were controlled by the same computer, so that administrations and blood sampling were synchronized.

Dosing Regimen

In order to have time for four observations (minimum time interval between observations was 15 min) with increasing concentrations a 2 h i.v. infusion was chosen for test compound administration. In a preliminary study with single bolus i.v. administrations of T, SS-T and RR-T, concentrations were identified at which about 80% of maximum pharmacological activity was achieved. Based on these data and taking the half-lives of the test compounds into account, infusion rates were calculated which would achieve about 80% of maximum activity at the end of the 2 h infusion.

Study Execution

Before start of administration of the test substance administration, baseline values of the pharmacological observations were recorded. Therefore aluminium plates, designed to fit in the RATURN® cages and cooled to 4°C in a refrigerator, were placed in the cages so that the rat was sitting on the cold surface. Brisk withdrawals of the right hind paw were counted for 2 min. From 30 to 40 brisk withdrawls were observed, which is well comparable to values obtained in non cannulated rats before start of substance administration. In addition a blank blood sample was taken, from which the haematocrit was determined.

Pharmacokinetics. Blood samples were taken at the following times after start the infusion of saline, T, SS-T or RR-T: 0.33, 0.66, 1.5, 1.9, 2.17, 2.55, 3.55, 4.55 and 6.05 h. After start of the infusion of either SS-M1 or RR-M1 the following sampling times were applied: 0.33, 0.58, 1.08, 1.5, 1.9 2.17, 2.55, 4.55 and 6.05 h. At every sampling time a volume of 180 μl of blood was taken by the "no waste blood" method. To obtain plasma, every vial was prepared with 18 μl of heparin saline (10 U/ml). In addition and to prevent clotting, 50 μl of isotonic saline with heparin (10 U/ml), used as system liquid in the tubing set of the Culex® automated blood sampling device, was added. The dilution factor for the samples of individual rats was calculated on the plasma content determined from the haematocrit. After centrifugation at 3,000×*g* for 5 min, plasma was stored at −80°C until analysis.

Pharmacodynamics. Assessment of pharmacodynamic effect was performed at the following times after start of the infusion of the test compound: 0.25, 0.5, 1, 1.85, 2.08, 2.5, 3.5, 4.5 and 6 h. Brisk withdrawals of the right hind paw were counted for 2 min and recorded. After the observation, the aluminium plates were placed back into the refrigerator. The temperature of the aluminium plated were determined by a surface thermometer before and after the observation of brisk withdrawals. The start temperature was 2.5°C and increased to 5°C due to the body heat of the rat. The room

temperature, throughout all experiments, was in the range of 21.5 to 24.5°C.

Bioanalytical Quantification of Concentrations

Stereoselective quantification of T and M1 was performed using a validated analytical LC-MS/MS method. Samples were analyzed using a PE Sciex LC-MS/MS system consisting of a Perkin Elmer HPLC pump (type series 200), a Perkin Elmer Autosampler (type series 200), coupled to a MDS/Sciex API 4000 triple quadrupole mass spectrometer, which was equipped with an atmospheric pressure chemical ionization (APCI) interface acting in positive mode (capillary temperature at 300°C). Multiple reaction monitoring scan type was used for ion detection. Instrument control and data acquisition was performed using the Analyst software version 1.4.1 (MDS/Sciex, Toronto/Canada). Sample preparation consisted of addition of the internal standard, D6-*O*-desmethyl-tramadol, and solid phase extraction. Chromatographic separation was achieved using a 250×4.6 mm, 10 μm Chiralpak column equipped with a Lichrospher 100 diol precolumn (40×4.0 mm, 5 μm), with an isocratic flow of *n*-hexane/ethanol/diethylamine (94/6/0.1, *v*/*v*/*v*) at a flow rate of 1 ml/min. Precision and accuracy ranged from: (1) 5.2 to 6.5% and 95.0 to 107% (RR-T), (2) 4.9 to 7.3% and 95.8 to 105% (SS-T), (3) 3.2 to 6.0% and 96.8 to 105% (RR-M1), and (4) 3.1 to 6.6 and 96.6 to 107% (SS-M1), respectively. The method showed linearity over the concentration ranges studied.

Data Analysis

The population approach using the software NONMEM version V with the first order conditional estimation method with INTERACTION was used for the analyses (17). Between-subject variability (BSV) was modelled exponentially. Residual variability was described with a combined error model consisting in an additive and a concentration-proportional term for the case of the pharmacokinetic observations, and with an additive error model for the case of the antinociceptive response.

Model selection was based mainly on the inspection of goodness of fit plots and the precision of the parameter estimates. The minimum value of the objective function (MOFV) provided by NONMEM served as a guide during model building. For two nested model a decrease in MOFV (Δ_{MOFV}) of 6.63 points for an added parameter is significant at the 0.01 level.

Model parameters are presented as the estimates together with their coefficients of variation [CV(%)].The degree of BSV was also expressed as CV(%).

The models selected were explored using the visual predictive check (18). Five hundred replicates were simulated and 0.05, 0.5, and 0.95 percentiles were used in conjunction with corresponding data to assess model performance. The agreement between model-based simulations and observed values was judged visually.

Pharmacokinetic data were analyzed first and then, the response data were fit using the individual pharmacokinetic parameter model estimates. Figure 1 shows the final pharmacokinetic/pharmacodynamic model describing the antinociceptive effect of tramadol.

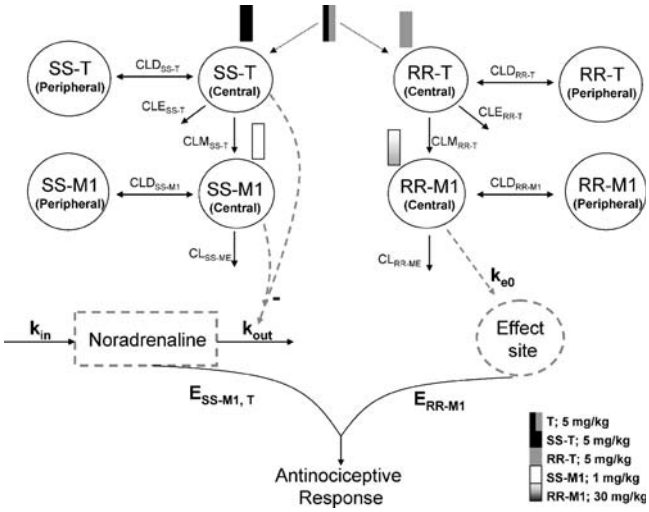

Fig. 1. Schematic representation of fthe final selected pk/pd model. Pharmacokinetics, Parent compounds (*RR-T*; *SS-T*): Vc, V_P, apparent volumes of distribution of the central and peripheral compartments; CL_D, intercompartmental clearance; CL_M, *O*-demethyltramadol formation clearance; CL_E, clearance of tramadol representing other routes of elimination. Metabolites (*RR-M1*; *SS-M1*): Vc_{M1}, and V_{PM1}, apparent volumes of distribution of the central and peripheral compartments; CL_{DM}, intercompartmental clearance; CL_{ME}, total plasma elimination clearance. Pharmacodynamics: k_{e0}, first order rate constant governing the equilibrium distribution of RR-M1 between plasma and the effect compartment; k_{in}, zero order rate constants of noradrenaline release; k_{out}, first order rate constant of noradrenaline re-uptake.

Pharmacokinetic analysis. Since it is well known that tramadol does not undergo enantiomer inter-conversion, data for each of the enantiomers were fit separately (4,7,8). Pharmacokinetic models were parameterized in apparent volumes of distribution and elimination clearances. One-, two-, and three-compartment models were fit to the parent drug and metabolite data. Metabolite formation was assumed to follow a first order process, and for the elimination of the parent drug models with one elimination pathway (M1 formation) or two elimination pathways (M1 formation + other routes of elimination) were compared. In group VI, SS-M1 was given at a dose five times higher that the doses administered to groups II and IV, and therefore models accounting for non-linear (concentration-dependent) kinetics in metabolite distribution and eliminations were also fitted when analyzing the data from the SS-enantiomers.

Pharmacokinetic/pharmacodynamic analysis. The model describing simultaneously the response data from the six groups of animals was built in two steps. First, the data from each group receiving enantiomer administration plus the data from the saline group were fit separately to identify the active components, and their functional relationship with the response. Then the interaction model was developed integrating the data from the group receiving racemic tramadol.

Models have the following general form:

$$E = E_0 \times E_{Saline} \times \left(1 - E_{Drug}\right) \quad (1)$$

[equation 1], where E, represents the observed response at any time, E_0, is the response level at baseline, E_{Saline} represents

the change in the response over time in the animals receiving saline, and E_{Drug} corresponds to a 0–1 normalized antinociceptive stimulus induced after drug administration.

Step I

Administration of saline. A constant (time independent) model and different empirical time-dependent models, including linear and non-linear increase/decrease in the response, as a function of the time after the start of the intravenous infusion of saline, were explored to select the best expression for E_{Saline}.

Administration of RR-M1. The effect compartment model (19) was used to link the predicted effect site concentration of RR-M1 ($C_{e\_RR\text{-}M1}$) with the antinociceptive stimulus ($E_{RR\text{-}M1}$) through the first order rate constant of equilibrium (k_{e0}), using the following expression:

$$E_{RR-M1} = \frac{\frac{C_{e\_RR-M1}}{IC_{50\_RR-M1}}}{1 + \frac{C_{e\_RR-M1}}{IC_{50\_RR-M1}}} \quad (2)$$

where $IC_{50\_RR\text{-}M1}$, is the steady-state plasma concentration of RR-M1 eliciting half of maximum stimulus.

Administration of SS-M1. SS-M1 is a monoamine re-uptake inhibitor (3) and its effects were described with an indirect response model (20):

$$\frac{dR}{dt} = kin - kout \times \left[1 - \frac{\frac{C_{SS-M1}}{IC_{50\_SS-M1}}}{1 + \frac{C_{SS-M1}}{IC_{50\_SS-M1}}}\right] \times R \quad (3)$$

where R, represents the arbitrary levels of noradrenaline in the biophase; k_{in}, and k_{out} are the zero, and first order rate constants of release and re-uptake of noradrenaline, respectively, and $IC_{50\_SS\text{-}M1}$, is the steady-state plasma concentration of SS-M1 ($C_{SS\text{-}M1}$) eliciting half of maximum reduction in k_{out}. The antinociceptive stimulus induced by SS-M1 ($E_{SS\text{-}M1}$) has the form: $E_{SS\text{-}M1}=(R-1)/R$. At time=0, R is equal to 1 and $E_{SS\text{-}M1}$ is equal to 0 (initial condition).

Administration of RR-Tramadol. The interaction between $C_{e\_RR\text{-}M1}$ and the effect site concentrations of RR-tramadol ($C_{e\_RR\text{-}T}$) was modelled with a competitive interaction model of the form:

$$E_{RR-M1,T} = \frac{\frac{C_{e\_RR-T}}{IC_{50\_RR-T}} + \frac{C_{e\_RR-M1}}{IC_{50\_RR-M1}}}{1 + \frac{C_{e\_RR-T}}{IC_{50\_RR-T}} + \frac{C_{e\_RR-M1}}{IC_{50\_RR-M1}}} \quad (4)$$

where $E_{RR\text{-}M1,T}$, is the antinociceptive stimulus corresponding to the combination of RR-M1, and RR-T, and $IC_{50\_RR\text{-}T}$, is the steady-state plasma concentration of RR-T eliciting half of maximum stimulus when RR-M1 is absent. An expression resembling the Bliss independence (21) was also fit to the data [Jonker et al. (22) (expression not shown)]. The results from this analysis showed that contribution of RR-T to the antinociceptive response was negligible.

Administration of SS-Tramadol. The interaction between SS-T and SS-M1 was described using the following expression (23) which corresponds to a competitive interaction mechanism:

$$\frac{dR}{dt} = kin - kout \times \left[1 - \frac{\frac{C_{SS-T}}{IC_{50\_SS-T}} + \frac{C_{SS-M1}}{IC_{50\_SS-M1}}}{1 + \frac{C_{SS-T}}{IC_{50\_SS-T}} + \frac{C_{SS-M1}}{IC_{50\_SS-M1}}}\right] \times R \quad (5)$$

where $IC_{50\_SS\text{-}T}$, is the steady-state plasma concentration of SS-T ($C_{SS\text{-}T}$) eliciting half of maximum reduction in k_{out}, when SS-M1 is absent. The antinociceptive stimulus induced by SS-T and SS-M1 in combination ($E_{SS\text{-}M1,T}$) has the form: $E_{SS\text{-}M1,T}=(R-1)/R$. At time=0, R is equal to 1 and $E_{SS\text{-}M1,T}$ is equal to 0 (initial condition).

Step II

The model used to describe the complete set of data including the observations after the administration of racemic tramadol characterising the type of the interaction between the μ-opioid and monoamine components of T effects, was based on the response surface analysis proposed by Minto *et al.* (24).

We define E_{RR}, and E_{SS} as ($C_{e\_RR\text{-}M1}/IC_{50\_RR\text{-}M1}$) and ($R-1$), respectively. The total stimulus is then the sum of E_{RR} and E_{SS}, and the contribution of each stimulus is given by:

$$D = \frac{E_{SS}}{E_{RR} + E_{SS}} \quad (6)$$

Finally, the antinociceptive stimulus resulted from the interaction between the active components of T ($E_{RR,SS}$) is represented by:

$$E_{RR,SS} = \frac{\frac{E_{RR}+E_{SS}}{E_{50}}}{1 + \frac{E_{RR}+E_{SS}}{E_{50}}} \quad (7)$$

where E_{50} is given by the following expression (24): $E_{50}=1-\theta\times D+\theta\times D^2$. The parameter θ to be estimated by the model determines the type of interaction: (1) if $E_{50}=1$ ($\theta=0$) the stimuli are additive, (2) if $E_{50}<1$ the interaction is synergistic, and (3) if $E_{50}>1$ the interaction is antagonistic.

Note that equation 7 reduces to equations 2–5 when RR-M1, RR-T, SS-M1, and SS-T are single administered.

RESULTS

Pharmacokinetic analysis. Both enantiomers of tramadol and M1 showed plasma concentration *vs* time profiles that were best described with a two-compartment model. The inclusion of a second elimination pathway was significant for RR-, and SS-T ($\Delta_{MOFV}=-11.0$; $P<0.01$). Weight exerted a significant ($\Delta_{MOFV}=-8.7$; $P<0.01$) covariate effect on Vc, the apparent volume of distribution of the central compartment, of RR-T, reducing BSV from 36 to 20%. The covariate model predicts an increase of 0.022 l for every 10 g increase in body weight. However for the rest of studied compounds SS-T, RR-, and SS-M1, weight effects were not significant ($\Delta_{MOFV}=-3.1$; $P>0.05$). Between-subject variability could be estimated

Table I. Population pharmacokinetic parameter of RR-, SS-Tramadol, and RR-, SS -*O*-demethyltramadol in the rat

	RR- enantiomers		SS- enantiomers	
Parameter	Typical population estimate	Between-subject variability	Typical population estimate	Between-subject variability
Vc(l)[a]	0.47 (15)	20 (33)	0.51 (28)	20 (32)
CL_E(l/h)	0.86 (19)	53 (26)	1.3 (11)	36 (15)
CL_M(l/h)	0.58 (15)	18 (29)	0.52 (12)	17 (22)
CL_D(l/h)	0.82 (29)		0.46 (71)	
V_P(l)	0.58 (12)		0.34 (28)	
Vc_{M1}(l)	0.52 (10)		1.1 (8)	
CL_{ME}(l/h)	2.7 (11)	28 (23)	2.2 (8)	20 (30)
CL_{DM}(l/h)	0.97 (31)		0.6 (10)	
V_{PM1}(l)	2.8 (61)		2.1 (38)	
Additive $error_{\_Parent}$ (ng/ml)	2.8 (29)		0.96 (46)	
Proportional $error_{\_Parent}$ (%)	13 (18)		21 (14)	
Additive $error_{\_Metabolite}$ (ng/ml)	2.1 (21)		1.3 (42)	
Proportional $error_{\_Metabolite}$ (%)	15 (21)		21 (10)	

Parameter estimates are listed with their coefficient of variation [CV(%)] in parenthesis, computed as the ratio between the standard error and the parameter estimate multiplied by 100. Estimates of between-subject variability are expressed as CV (%). Parameters are defined in the text and in the legend to Fig. 1.

[a] Vc for the case of RR-Tramadol has the expression of 0.47×weight/220, where 220 is the mean animal body weight.

in Vc, CL_M (M1 formation clearance), CL_E (plasma clearance representing other routes of elimination of tramadol), and CL_{ME} (total plasma clearance of M1).

Table I lists the estimates of the pharmacokinetic model parameters for the each enantiomer of tramadol and M1, respectively. Parameters were estimated with good precision. Figures 2 and 3 show how the model describes the data of the RR- and SS-enantiomers, respectively, based on the results obtained from the visual predictive check. The mean population tendencies are very well captured by the model, as well as the variability in the data.

The typical population pharmacokinetic profiles of the enantiomers of tramadol and M1 are presented in Fig. 4 for comparison. Plasma disposition appears similar between enantiomers.

Pharmacokinetic/Pharmacodynamic Analysis

Step I

Administration of saline. Response data in the saline group showed a slight but significant decrease with time (Δ_{MOFV}= −15.3; P<0.01), that was described with a linear model using equation 1 with the following expression for E_{Saline}: 1-Slope x time. Other models such a biexponential model or an exponential decrease model did not improve the fit significantly (Δ_{MOFV}=−2.8; P>0.05) with respect to the linear model.

Administration of RR-M1. The time course of response was described properly using the model represented by equation 2. The use of the plasma concentrations instead of the effect site levels provided a significantly worse description of the data (Δ_{MOFV}=−30.4; P<0.01). The data supported between-subject variability in E_0 and $IC_{50RR\text{-}M1}$ with estimates, expressed as coefficient of variation, of 14% and 41%, respectively. The typical population estimates of E_0, k_{e0} (h^{-1}) and $IC_{50RR\text{-}M1}$ (ng/ml) were 33.5, 3.5, and 17.1, respectively.

Administration of SS-M1. A model relating directly the plasma concentrations of SS-M1 with the observed response resulted in a significantly worse description of the data compared to the model in equation 3 (Δ_{MOFV}=−28.7; P< 0.01). The typical population estimates of E_0, k_{out} (h^{-1}) and $IC_{50SS-M1}$ (ng/ml) were 32.9 3.96, and 858, respectively. Between-subject variability showed only significance in E_0 (14%; Δ_{MOFV}=−9.1; P<0.01).

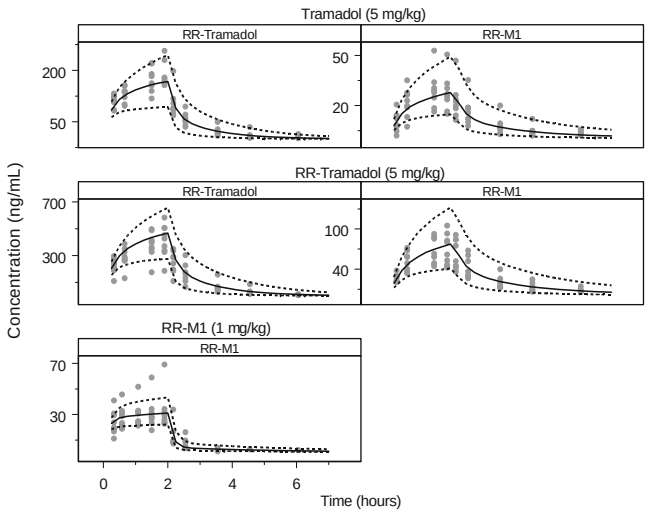

Fig. 2. Concentration *vs* time profiles of RR-Tramadol and RR-M1. Symbols represent raw data. The *solid lines* are the median pharmacokinetic profiles obtained from 500 simulated animals. The *dashed lines* cover the areas corresponding to the 90% of the simulated concentrations.

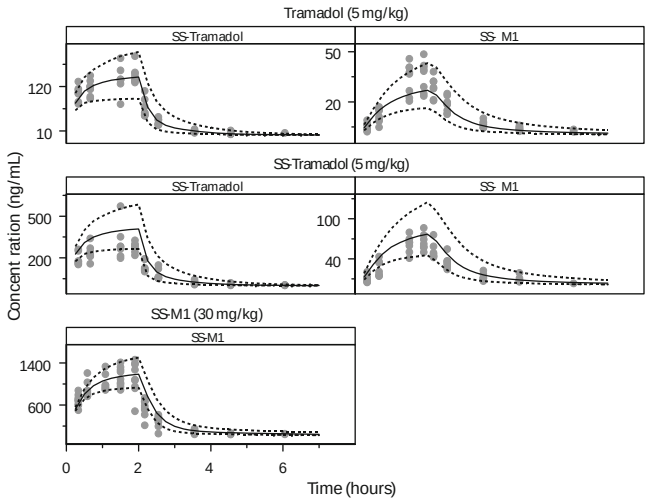

Fig. 3. Concentration *vs* time profiles of SS-Tramadol and SS-M1. *Symbols* represent raw data. The *solid lines* are the median pharmacokinetic profiles obtained from 500 simulated animals. The *dashed lines* cover the areas corresponding to the 90% of the simulated concentrations.

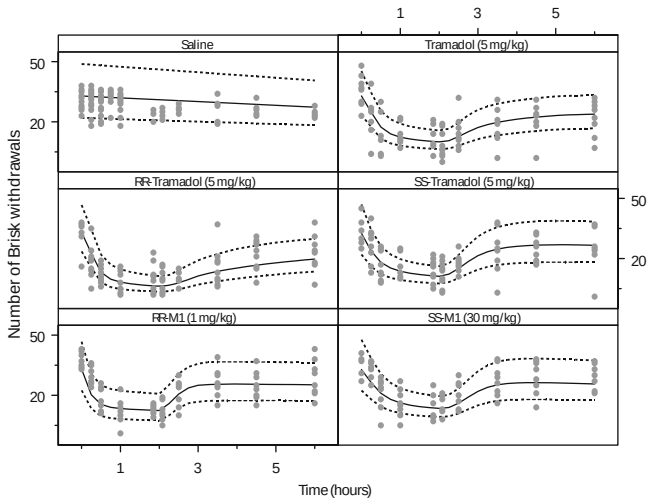

Fig. 5. Response *vs* time profiles. *Symbols* represent raw data. The *solid lines* are the median pharmacodynamic profiles corresponding to the selected interaction model and obtained from 500 simulated animals. The *dashed lines* cover the areas corresponding to the 90% of the simulated observations.

Administration of RR-Tramadol. The model represented by equation 4 did not perform significantly better than the model considering RR-M1 the only active component (equation 2; $\Delta_{MOFV}=-0.000$; $P<0.05$). The typical population estimates of E_0, k_{e0} (h^{-1}) and $IC_{50\_RR\text{-}M1}$ (ng/ml) were 32.2, 3.73, and 19.1, respectively. The degree of between-subject variability estimated for E_0 and $IC_{50RR\text{-}M1}$ was 15% and 23%, respectively.

Administration of SS-Tramadol. The competitive interaction model in equation 5 provided a good description of the data and gave precise estimates of the model parameters. The typical estimates of E_0, k_{out} (h^{-1}) and $IC_{50\_SS\text{-}M1}$ (ng/ml) were 31.3, 3.7 and 840, respectively, and the estimate of $IC_{50\_SS\text{-}T}$ was 230 (ng/ml). Variability in E_0 was estimated in 18%.

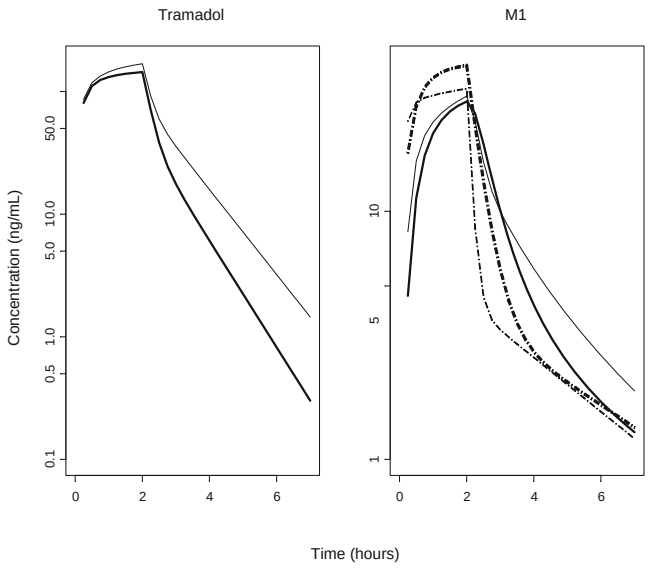

Fig. 4. Typical model predicted concentration *vs* time profiles for tramadol (*left panel*) and M1 (*right panels*). Thin and thick lines represent the kinetics of the RR-, and SS-enantiomers. In the *right panel solid lines* represent the kinetics of M1 after administration of racemic tramadol (dose=5 mg/kg), and *dashed lines* the kinetics of M1 after the administration of the metabolites alone (dose=0.8 mg/kg).

Step II

When the interaction model between the two different types of stimuli represented by equation 7 was fit to the data from all the six groups of animals, the estimate of the interaction parameter θ was 2.85×10^{-5}, and not significantly different from 0 ($\Delta_{MOFV}=0.000$; $P>0.05$). Figure 5 shows that all data for all groups in the study were described very well by the selected interaction model represented in equation 7 with $E_{50}=1$, since mean tendencies and dispersion in the data were adequately captured by the simulated profiles. Table II lists the values of the population pharmacodynamic model parameters, where it can be observed that all estimates have good precision. The antinociceptive stimuli *vs* steady-state

Table II. Population pharmacodynamic parameters of tramadol and *O*-demethyltramadol enantiomers in the rat

Parameter	Typical population estimate	Between-subject variability
E_0 (n° of brisk withdrawals)	33 (3)	19 (17)
Slope (1/h)	0.028 (17)	
$IC_{50\_RR\text{-}M1}$ (ng/ml)	20.2 (11)	32 (49)
k_{e0} (h^1)	5.04 (30)	
k_{out} (h^1)	5.5 (20)	
$IC_{50\_SS\text{-}T}$ (ng/ml)	230 (12)	
$IC_{50\_SS\text{-}M1}$ (ng/ml)	869 (12)	
Residual error (n° of brisk withdrawals)	4.98 (0.5)	

Parameter estimates are listed with their coefficient of variation [CV (%)] in parenthesis, computed as the ratio between the standard error and the parameter estimate multiplied by 100. Estimates of between-subject variability are expressed as CV (%). Parameters are defined in the text.

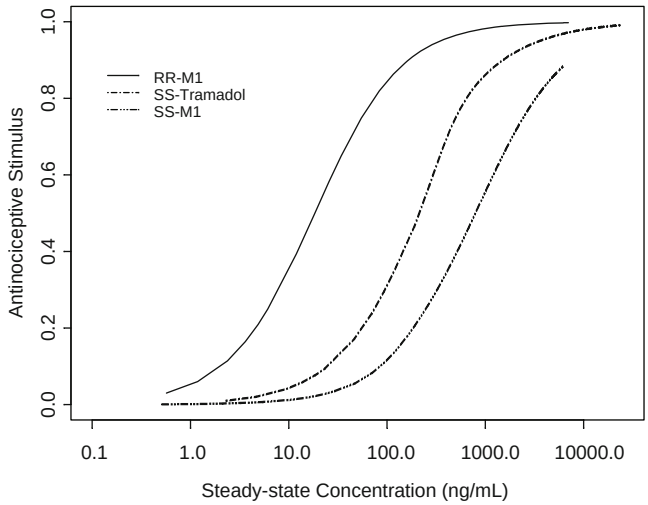

Fig. 6. Antinociceptive stimulus *vs* steady state plasma concentrations for each of the active components identified.

concentration relationship for the three active components identified in the current analysis and predicted by the selected model, is presented in Fig. 6.

The kinetic profiles of the two main active components of tramadol together with their corresponding stimuli are shown in Fig. 7. Despite plasma concentrations of RR-M1 are much lower than $C_{SS\text{-}T}$, the antinociceptive stimulus of RR-M1 is still greater that the one elicited by SS-T.

DISCUSSION

A semi-mechanistic pk/pd model integrating the different pharmacological mechanisms of T has been established in healthy conscious freely-moving rats fulfilling the major goal of the current study.

The experimental setup used in this work combines automated blood sampling device and the Bennett model of neuropathic pain with cold allodynia as readout. This approach has the advantage of being less stressful for the animals allowing to almost, synchronize blood sampling and pharmacological observations reducing direct contact with the animal to a minimum, and increasing the reliability of the pharmacological data.

Taking into consideration the multiple pharmacological mechanisms of T, the choice of an adequate pain model represents a critical step, since not all models available are suitable in reflecting all aspects of T activity. For example, it is well known that the tail-flick test is very appropriate to characterize the μ-opioid activity, but it generally fails to demonstrate other mechanisms such as the contribution of the monoamine re-uptake inhibition. The method used in this study has several advantages. First, it can reflect anti-allodynic effects mediated by opioid receptor binding, and monoamine re-uptake inhibition (14). Second, the Bennett model is established as a pharmacological model for chronic neuropathic pain displaying a very stable baseline response over a period of weeks after surgery. Third, from pk/pd modelling perspective this animal model provides continuous decreasing response with respect to baseline, which means that it has a natural maximum effect (E=0) facilitating the estimation of the C_{50} parameters in contrast with other pain models, where the response is usually modelled as linear relationship with respect to drug exposure (8,25).

One important aspect in pk/pd modelling is dosing and data acquisition. Based on a preliminary investigation, an infusion design was calculated providing concentration profiles covering the full range of the pharmacodynamic observations [which explains the reason for a reduced dose of RR-M1 (1 mg/kg) and the increased dose of SS-M1 (30 mg/kg) compared with the dose for T and its enantiomers (5 mg/kg)] with the absence of relevant adverse effects. Figure 5 confirms that the final dosing regimens used produced response profiles that achieved 90% of the maximum possible effect, recovering the baseline conditions at the end of the observation period.

The population pk model was able to describe the enantiomers data of T and M1 regardless which entity was administered, T, RR-/SS-T, or RR-/SS-M1. The typical

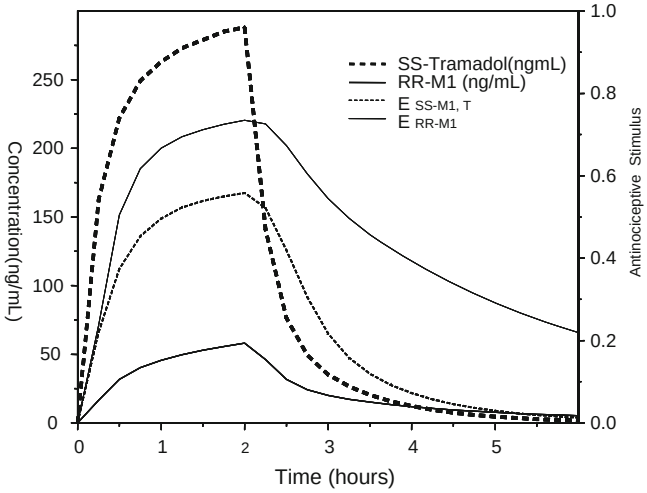

Fig. 7. Simulated plasma concentration of SS-Tramadol and RR-M1 *vs* time profiles together with their corresponding antinociceptive stimulus after a 10 min intravenous infusion of 10 mg/kg of racemic tramadol.

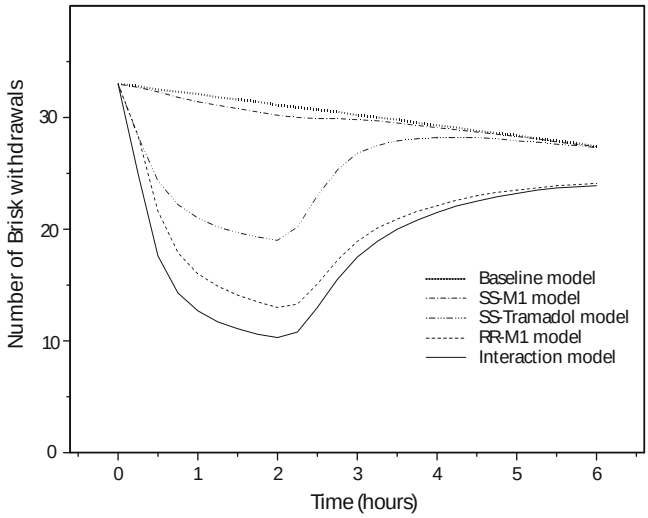

Fig. 8. Simulated response *vs* time profiles corresponding to the baseline, SS-M1, SS-Tramadol, RR-M1 and the (final) interaction models.

population estimates of CL, computed as the sum of CL_M and CL_E, are comparable to the estimates published previously [2.04 and 1.9 l/h for RR-/SS-M1, respectively (4)], as well as the typical estimates of the apparent volume of distribution of the central compartment. The typical estimates of apparent volume of distribution of the peripheral compartment are greater, 2.8 and 2.1 l, than those reported previously [0.6–1 l (4,7,8)]. The reason for such discrepancy might be the fact that the blood sampling period after the end of administration was significantly prolonged in the current study [6 *vs* 1–3 h in the previous studies], providing a better characterisation of the terminal disposition phase. With respect to the pharmacokinetics of the parent compound, it seems that the metabolic pathway dealing with the formation of M1 plays an important role in the elimination process accounting for 28–40% of the total value of plasma clearance.

Simulations presented in Fig. 4 show that after racemic administration of tramadol the plasma concentrations for RR-T and RR-M1 are slightly higher than the corresponding for the SS enantiomers, a result that has also been seen in clinical studies (13). Lastly, enantiomers of T and M1 show a low to moderate degree of between-subject variability in the pk parameters ranging from 17 to 53%.

The integrated pk/pd model combines four types of sub-models, (1) a sub-model for time effects after saline administration, (2) a sub-model accounting for μ-opioid mediated effects, (3) a sub-model describing the effects resulting from the inhibition of monoamine re-uptake (this model also involves a competitive interaction between the SS-T and SS-M1), and (4) a sub-model dealing with the interaction on the antinociceptive response between the μ-opioid and monoamine related effects.

The model used to describe the μ-opioid has been used in the past for different opioid drugs (7,25) using different animal models. The lack of pharmacodynamic interaction between RR-T and RR-M1 was an expected result based on previous pk/pd results (8). RR-M1 was found the unique component acting at the level of the μ-receptor. Interestingly, the estimates of k_{e0} for RR-M1 found in this study are very similar to those reported previously, where the tail flick was used as the experimental pain model (4,7). Direct comparison between the parameters reflecting drug potency is difficult because of the use of a linear pd model in previous articles. We have to emphasize that the parameter k_{e0}, although defined as the first order rate constant governing the distribution equilibrium delay between plasma and effect site, might be also reflecting receptor coupling and signal transduction processes.

The sub-model used to describe the effect of the SS-enantioners was based on known pharmacological mechanism where k_{out} is defined as the first order rate of nordrenaline re-uptake. However and since noradrenaline was not experimentally measured, the mechanistic interpretation of the estimate of k_{out}, as in the case of k_{e0}, should be done with caution. Since both compounds share the same mechanism, a competitive model accounting for the interaction between the two compounds seems to be the natural choice. SS-M1 resulted in a much less potent compound, in fact its contribution to the overall effect after administration of racemic tramadol can be considered negligible. The ratio between the IC_{50} estimates for SS-M1 and SS-T has a value of 3.8, which is very similar to the ratio that can be derived from the Ki (mol/l) values of SS-M1 (1.8×10^{-6}) and SS-T (5.9×10^{-7}) calculated from *in vitro* data of NA uptake inhibition (3) which is 3.05. Regarding RR-M1 we computed the ratio between its IC_{50} (20.2 ng/ml) and the IC_{50} of SS-T (230 ng/ml) resulting a value of 0.088. A result close to the value obtained from the Ki ratio between RR-M1 [μ-receptor *in vitro* activity (2.2×10^{-8})] and SS-T [*in vitro* data of NA uptake inhibition (5.9×10^{-7})] which is 0.04 (3). These findings support the mechanistic characteristic of the proposed model.

Finally, Fig. 8 shows the contribution of the baseline, SS-M1, SS-T, and RR-M1 effects to the response profiles after a 2 h intravenous infusion of 5 mg/kg of racemic tramadol based on the model estimates listed in Table II. Effects of SS-M1 are negligible, and SS-T contributes slightly to the response mediated by RR-M1. This plots shows also that tramadol effects would not be completely abolished in the case of poor formation of M1, implying that completed blockade of the RR-M1 formation pathway would not abolish totally the effects of tramadol, as it has been seen in the case of clinical data (26). Administration of higher doses of tramadol in an attempt to overcome the hypoalgesic effects of a reduction in RR-M1 formation would not be indicated because of the increase rate of adverse effects. This important issue has not been addressed in the current study, and will the natural continuation with the goal of establish the utility function of tramadol at different degrees of RR-M1 formation inhibition.

Although μ-opioid receptor expression has been shown to be reduced in neuropathic pain states in animals (27), μ-opioid receptor agonists show analgesic efficacy in neuropathic pain in rodents (14,16) and human (28–30). On the other hand, monoaminergic mechanisms at spinal and supraspinal levels are thought to be the basis of analgesic efficacy of antidepressants in neuropathic pain (31). The combination of both mechanisms could be the basis for the excellent efficacy of tramadol in neuropathic pain states in animals (14) and human (32).

The interaction between the μ-receptor and monoaminergic mechanisms was described empirically using a response surface analysis (24,33) and resulted to be additive, although it would be also possible to find a different class of interaction using other animal models of pain. In addition and taking into consideration the recent published experimental design for drug combination studies, the dose range used in the current analysis (34) can be considered limited.

To summarize the results, a semi-mechanistic pk/pd model has been developed for the tramadol effects *in vivo*. The model predicts that RR-M1 is the major active element but SS-T contributes significantly. Our study also that the Bennett model is a suitable model for drugs exerting their action through the opioid and monoamine re-uptake inhibition systems.

ACKNOWLEDGMENTS

We like to thank Manuela Graff, Elke Schumacher, Johanna Korioth and Carolin Koll for excellent technical support. The contribution of Norbert Bromet, Biotec Centre (Orleans, France) to the bioanalytical determination of drug concentrations in plasma is greatly appreciated.

REFERENCES

1. R. B. Raffa, E. Friderichs, W. Reimann, R. P. Shank, E. E. Codd, and J. L. Vaught. Opioid and nonopioid components independently contribute to the mechanism of action of tramadol, an 'atypical' opioid analgesic. *J Pharmacol Exp Ther* **260**:275–285 (1992).
2. H. H. Hennies, E. Friderichs, and J. Schneider. Receptor binding, analgesic and antitussive potency of tramadol and other selected opioids. *Arzneimittelforschung* **38**:877–880 (1988).
3. M. C. Frink, H. H. Hennies, W. Englberger, M. Haurand, and B. Wilffert. Influence of tramadol on neurotransmitter systems of the rat brain. *Arzneimittelforschung* **46**:1029–1036 (1996).
4. M. J. Garrido, M. Valle, M. A. Campanero, R. Calvo, and I. F. Troconiz. Modeling of the *in vivo* antinociceptive interaction between an opioid agonist, (+)-*O*-desmethyltramadol, and a monoamine reuptake inhibitor, (-)-*O*-desmethyltramadol, in rats. *J Pharmacol Exp Ther* **295**:352–359 (2000).
5. B. Driessen, W. Reimann, and H. Giertz. Effects of the central analgesic tramadol on the uptake and release of noradrenaline and dopamine *in vitro*. *Br J Pharmacol* **108**:806–811 (1993).
6. T. A. Bamigbade, C. Davidson, R. M. Langford, and J. A. Stamford. Actions of tramadol, its enantiomers and principal metabolite, O-desmethyltramadol, on serotonin (5-HT) efflux and uptake in the rat dorsal raphe nucleus. *Br J Anaesth* **79**:352–356 (1997).
7. M. Valle, M. J. Garrido, J. M. Pavon, R. Calvo, and I. F. Troconiz. Pharmacokinetic-pharmacodynamic modeling of the antinociceptive effects of main active metabolites of tramadol, (+)-*O*-desmethyltramadol and (-)-*O*-desmethyltramadol, in rats. *J Pharmacol Exp Ther* **293**:646–653 (2000).
8. M. J. Garrido, O. Sayar, C. Segura, J. Rapado, M. C. Dios-Vieitez, M. J. Renedo, and I. F. Troconiz. Pharmacokinetic/pharmacodynamic modeling of the antinociceptive effects of (+)-tramadol in the rat: role of cytochrome P450 2D activity. *J Pharmacol Exp Ther* **305**:710–718 (2003).
9. D. Le Bars, M. Gozariu, and S. W. Cadden. Animal models of nociception. *Pharmacol Rev* **53**:597–652 (2001).
10. M. J. Garrido, W. Habre, F. Rombout, and I. F. Troconiz. Population pharmacokinetic/pharmacodynamic modelling of the analgesic effects of tramadol in pediatrics. *Pharm Res* **23**:2014–2023 (2006).
11. R. S. Pedersen, P. Damkier, and K. Brosen. Tramadol as a new probe for cytochrome P450 2D6 phenotyping: a population study. *Clin Pharmacol Ther* **77**:458–467 (2005).
12. S. Laugesen, T. P. Enggaard, R. S. Pedersen, S. H. Sindrup, and K. Brosen. Paroxetine, a cytochrome P450 2D6 inhibitor, diminishes the stereoselective O-demethylation and reduces the hypoalgesic effect of tramadol. *Clin Pharmacol Ther* **77**:312–323 (2005).
13. L. Poulsen, L. Arendt-Nielsen, K. Brosen, and S. H. Sindrup. The hypoalgesic effect of tramadol in relation to CYP2D6. *Clin Pharmacol Ther* **60**:636–644 (1996).
14. T. Christoph, B. Kögel, W. Strassburger, and S. A. Schug. Tramadol has a better potency ratio relative to morphine in neuropathic than in nociceptive pain models. *Drugs R D* **8**:51–57 (2007).
15. G. J. Bennett, and Y. K. Xie. A peripheral mononeuropathy in rat that produces disorders of pain sensation like those seen in man. *Pain* **33**:87–107 (1988).
16. T. Christoph, B. Kögel, K. Schiene, M. Méen, J. De Vry, and E. Friederichs. Broad analgesic profile of buprenorphine in rodent models of acute and chronic pain. *Eur J Pharmacol* **507**:87–98 (2005).
17. S. L. Beal, and L. B. Sheiner. NONMEM User's Guides. San Francisco: NONMEM Project Group. University of California, 1998.
18. N. H. Holford. The visual Predictive Check - Superiority to Standard Diagnostic (Rorschach) Plots. PAGE 14 Abstr 738 (2005).www.page-meeting.org/?abstract=738
19. L. B. Sheiner, D. R. Stanski, S. Vozeh, R. D. Miller, and J. Ham. Simultaneous modeling of pharmacokinetics and pharmacodynamics: application to d-tubocurarine. *Clin Pharmacol Ther* **25**:358-371 (1979).
20. N. L. Dayneka, V. Garg, and W. J. Jusko. Comparison of four basic models of indirect pharmacodynamic responses. *J Pharmacokinet Biopharm* **21**:457–478 (1993).
21. C. I. Bliss. The toxicity of poissons applied jointly. *Ann Appl Biol* **26**:585–615 (1939).
22. D. M. Jonker, S. A. Visser, P. H. van der Graaf, R. A. Voskuyl, and M. Danhof. Towards a mechanism-based analysis of pharmacodynamic drug–drug interactions *in vivo*. *Pharmacol Ther* **106**:1–18 (2005).
23. J. Earp, W. Krzyzanski, A. Chakraborty, M. K. Zamacona, and W. J. Jusko. Assessment of drug interactions relevant to pharmacodynamic indirect response models. *J Pharmacokinet Pharmacodyn* **31**:345-380 (2004).
24. Ch. F. Minto, T. W. Schinder, T. G. Short, K. M. Gregg, A. Gentilini, and S. L. Shafer. Response surface model for anesthetic drug interactions. *Anesthesiology* **92**:1603–1616 (2000).
25. M. Gårdmark, and M. Hammarlund-Udenaes. Delayed antinociceptive effect following morphine-6-glucuronide administration in the rat-pharmacokinetic/pharmacodynamic modelling. *Pain* **74**:287–296 (1998).
26. T. P. Enggaard, L. Poulsen, L. Arendt-Nielsen, K. Brosen, J. Ossig, and S. H. Sindrup. The analgesic effect of tramadol after intravenous injection in healthy volunteers in relation to CYP2D6. *Anesth Analg* **102**:146–150 (2006).
27. M. H. Rashid, M. Inoue, K. Toda, and H. Ueda. Loss of peripheral morphine analgesia contributes to the reduced effectiveness of systemic morphine in neuropathic pain. *J Pharmacol Exp Ther* **309**:380–387 (2004).
28. P. L. Dellemijn, and J. A. Vanneste. Randomised double-blind active-placebo-controlled crossover trial of intravenous fentanyl in neuropathic pain. *Lancet* **349**:753–758 (1997).
29. J. S. Gimbel, P. Richards, and R. K. Portenoy. Controlled-release oxycodone for pain in diabetic neuropathy: A randomized controlled trial. *Neurology* **60**:927–934 (2003).
30. C. P. Watson, and N. Babul. Efficacy of oxycodone in neuropathic pain: a randomized trial in postherpetic neuralgia. *Neurology* **50**:1837–1841 (1998).
31. J. A. Mico, D. Ardid, E. Berrocoso, and A. Eschalier. Antidepressants and pain. *Trends Pharmacol Sci* **27**:348–354 (2006).
32. R. M. Duhmke, D. D. Cornblath, and J. R. Hollingshead. Tramadol for neuropathic pain. *Cochrane Database Syst Rev* **2**: CD003726 (2004).
33. D. M. Jonker, R. A. Voskuyl, and M. Danhof. Pharmacodynamic analysis of the anticonvulsant effects of Tiagabine and Lamotrigine in combination in the rat. *Epilepsia* **45**:424–435 (2004).
34. T. Ch. Chou. Theoretical basis, experimental design, and computerized simulation of synergism and antagonism in drug combination studies. *Pharmacol Rev* **58**:621–681 (2006).